Acta Pharmaceutica Sinica B 2022;12(9):3667–3681

Chinese Pharmaceutical Association
Institute of Materia Medica, Chinese Academy of Medical Sciences

Acta Pharmaceutica Sinica B

www.elsevier.com/locate/apsb
www.sciencedirect.com

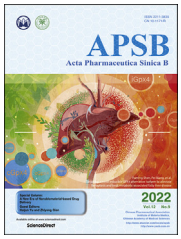

ORIGINAL ARTICLE

Small molecule SMU-CX24 targeting toll-like receptor 3 counteracts inflammation: A novel approach to atherosclerosis therapy

Xiaohong Cen[a], Baoqu Wang[a], Yuqing Liang[a], Yanlin Chen[a], Yu Xiao[a], Shaohua Du[b], Kutty Selva Nandakumar[a], Hang Yin[c,*], Shuwen Liu[a,*], Kui Cheng[a,b,*]

[a]*Guangdong Provincial Key Laboratory of New Drug Screening and State Key Laboratory of Organ Failure Research, School of Pharmaceutical Sciences, Southern Medical University, Guangzhou 510515, China*
[b]*Department of Musculoskeletal Oncology, the Third Affiliated Hospital of Southern Medical University, Guangzhou 510642, China*
[c]*School of Pharmaceutical Sciences, Beijing Advanced Innovation Center for Structural Biology, Tsinghua-Peking Joint Center for Life Sciences, Tsinghua University, Beijing 100084, China*

Received 28 March 2022; received in revised form 15 May 2022; accepted 26 May 2022

KEY WORDS

Toll-like receptor 3;
Atherosclerosis;
Small molecule;
Inflammation;
Macrophage

Abstract Toll-like receptor 3 (TLR3), as an important pattern recognition receptor (PRR), dominates the innate and adaptive immunity regulating many acute and chronic inflammatory diseases. Atherosclerosis is proved as an inflammatory disease, and inflammatory events involved in the entire process of initiation and deterioration. However, the contribution of TLR3 to atherosclerosis remains unclear. Herein, we identified the clinical relevance of TLR3 upregulation and disease processes in human atherosclerosis. Besides, activation of TLR3 also directly led to significant expression of atherogenic chemokines and adhesion molecules. Conversely, silencing TLR3 inhibited the uptake of oxLDL by macrophages and significantly reduced foam cell formation. Given the aberrance in TLR3 functions on atherosclerosis progression, we hypothesized that TLR3 could serve as novel target for clinical atherosclerosis therapy. Therefore, we developed the novel ellipticine derivative SMU-CX24, which specifically inhibited TLR3 (IC_{50} = 18.87 ± 2.21 nmol/L). *In vivo*, atherosclerotic burden was alleviated in Western diet fed $ApoE^{-/-}$ mice in response to SMU-CX24 treatment, accompanying notable reductions in TLR3 expression and inflammation infiltration within atherosclerotic lesion. Thus, for the first time, we revealed that pharmacological downregulation of TLR3 with specific inhibitor regenerated inflammatory environment to counteract atherosclerosis progression, thereby proposing a new strategy and probe for atherosclerosis therapy.

*Corresponding authors.
E-mail addresses: yin_hang@tsinghua.edu.cn (Hang Yin), Liusw@smu.edu.cn (Shuwen Liu), Chengk@smu.edu.cn (Kui Cheng).
Peer review under responsibility of Chinese Pharmaceutical Association and Institute of Materia Medica, Chinese Academy of Medical Sciences.

https://doi.org/10.1016/j.apsb.2022.06.001

1. Introduction

Cardiovascular diseases (CVDs) are multifactorial disorders affecting heart and cerebral vessel function, and remain one of the most life-threatening diseases in the world[1,2]. Among them, atherosclerosis (AS), which is characterized by lipid metabolism and inflammation disorders, is the main underlying pathological process that induces severe cardiac events, such as myocardial infarction and ischemic stroke. Atherosclerosis is proved as an inflammatory disease, and inflammatory events are involved in the entire process of initiation and deterioration[3,4]. As the most significant pattern recognition receptors (PRRs) in the immune system, Toll-like receptors (TLRs) recognize both pathogen-associated molecular patterns (PAMPs) and danger-associated molecular patterns (DAMPs), including exogenous microbes and endogenous harmful substances[5−7], to defend against attack. Since TLRs also regulate a wide range of cells in the cardiovascular system and vessel-specific expression of distinct TLRs is also observed in human arteries[8], TLRs mechanistically link inflammation and atherosclerosis[9,10]. In this pathophysiological event, a sustained release of ligands by plaque lesions and infectious substances, such as lipoproteins and nucleic acid derivatives, are detected by TLRs and facilitate excessive inflammatory responses, which culminate in cardiovascular dysfunction and atherosclerosis worsening[2,11]. Therefore, in addition to classical statin treatment, drug interventions to control lesion inflammation and the infiltration of immune cells by specifically targeting TLRs are proposed for atherosclerosis therapy.

TLR3 is largely localized in the endosomal membrane and recognizes double-stranded RNA (dsRNA). TLR3 initiates mainly NF-κB and type I interferon signaling cascades in response to viral infections through the adaptor protein TRIF[12,13]. Within the complex pathological process of atherosclerosis, a substantial release of endogenous RNA by inflamed tissues and necrotic cells occurs in the lesions, which constitutes a complex atherosclerotic inflammatory environment[14,15]. Components of the host response to viruses are also implicated in the pathogenesis of atherosclerosis[16−19]. In addition, exposure to the exogenous TLR3 agonist Poly I:C also exacerbated atherosclerotic lesions with abundant plaque accumulation due to arterial injury and imbalanced lipid metabolism in hypercholesterolemic mice[20−22]. Deficiency of the *Tlr3* gene attenuated atherosclerosis pathogenesis with narrow plaque and conferred arterial protection[23−25]. In this study, substantial evidence also highlights the atherogenic and proinflammatory role of TLR3. We have identified the presence of TLR3 colocalized macrophages, endothelial cells and smooth muscle cells in human atherosclerotic lesion. Significant upregulation of TLR3 in PBMC specimens from atherosclerosis patients compared to those from healthy donors also observed. In mice, TLR3 activation induced a dramatic increase in the expression of atherogenic chemokines and adhesion molecules that promoted foam cells, and silencing of *Tlr3* inhibited the oxidized low-density lipoprotein (oxLDL) induced foam cell formation macrophages, demonstrating the crucial role of TLR3 in atherosclerosis regulation. Hence, inhibiting TLR3 could be a potential strategy for atherosclerosis treatment, but the lack of TLR3-specific inhibitors has hindered further pharmacological research and development.

Recently, currently available TLR3 inhibitors have been mostly summarized by Federico et al.[26]. Among them, several TLR3 inhibitors, such as melatonin (TLR3/4 inhibitor), the HMG-CoA reductase inhibitor fluvastatin (TLR2/3/4/8 antagonist), and the anti-inflammatory agent oleanolic acid acetate, also exhibit significant cardio-protection. However, poor efficacy and specificity for TLR3 have prevented their use in clinical practice. Therefore, we designed, synthesized and evaluated a novel TLR3 inhibitor with high efficacy and specificity against atherosclerosis. In our previous studies, several novel small molecule TLR modulators, such as the TLR2 agonist SMU-Z1[27] and the commercially available TLR3 inhibitor CU-CPT 4a[28] were discovered using a cell-based high-throughput screening (HTS) strategy. In this study, we screened 15,700 compounds from the NCI and Maybridge libraries with a cell-based HTS method, and for the first time, we identified the carbazole compound 9-methyoxy-elliciptine (NSC69187), which exhibited TLR3-specific inhibitory effects. Further chemical optimization of 9-methyoxy-elliciptine to improve its efficacy and structural novelty was conducted. Extensive structure−activity relationship studies yielded the novel ellipticine derivative, SMU-CX24 with an IC_{50} value of 18.87 ± 2.21 nmol/L. SMU-CX24 is 10 times better than the parent compound in inhibiting TLR3 in a highly specific manner. Mechanistic studies verified the function of SMU-CX24 in decreasing Poly I:C-induced expression of adaptor proteins and inflammatory cytokine production by attenuating the NF-κB, IFN and MAPK signaling pathways. In addition, SMU-CX24 significantly inhibited proatherogenic chemokine synthesis and the expression of adhesion molecules, and decreased of the ox-LDL uptake and foam cell formation in macrophages. Treatment with SMU-CX24 alleviated atherosclerotic progression, decreased lesion burden and significantly reduced inflammatory infiltration induced by TLR3 deficiency in Western diet-fed $ApoE^{-/-}$ mice. These data demonstrated that SMU-CX24 was a notable TLR3 specific inhibitor that exerted its anti-inflammatory effects and protected against atherosclerosis in mice. Collectively, we revealed the biological relevance in TLR3 expression and atherosclerosis and provided insight into the underlying therapeutic potential of a novel specific TLR3 inhibitor (SMU-CX24) that mediated inflammation inhibition, which presented a new strategy for atherosclerosis therapeutic development and chemical probes to examine TLR3 in different pathogenesis processes.

2. Materials and methods

2.1. Human specimens and animals

Sections of the popliteal artery with abundant plaque were isolated from arteriosclerosis obliterans (ASO) patients after surgical excision in The Third Affiliated Hospital of Southern Medical University (Guangzhou, China). Specimens were fixed in 4% formalin

and histological cross-sections of plaque regions were indicated to subsequent HE staining, immunohistochemical and immunofluorescence analyses. The following primary antibody specific for rabbit-TLR3 (1:1000, ab137722, Abcam), rabbit CD31 antibody (1:1000, ab182981, Abcam), mouse α-SMA antibody (1:1000, ab7817, Abcam) and mouse CD68 antibody (1:1000, ab201340, Abcam) were used. The secondary antibody was Alexa Fluor 488 donkey anti-mouse IgG (H + L) (1:400, A21202, Invitrogen) and Alexa Fluor 594 donkey anti-rabbit IgG (H + L) (1:400, A21207, Invitrogen). Sodium heparin-treated blood specimens was collected from patients with severe atherosclerosis or healthy volunteers were collected from Neurology Department of Nanfang Hospital of Southern Medical University (Guangzhou, China). PBMC were isolated using ficoll density gradient centrifugation (LTS1077, TBD Science). All the participants were informed possible consequences and given consent to enroll in this work, and they had no prior history of autoimmune or immunodeficiency diseases that might likely alter TLR3 expression. All the experiments were conducted in accordance with institutionally approved protocols and guidelines. Eight-weeks old C57BL/6J wild type (male, 18−22 g) mice and SD rats (male, 250−300 g) were purchased from Southern Medical University experimental animal center (Guangzhou, China). Apolipoprotein E-deficient mice ($ApoE^{-/-}$ with C57BL/6J genetic background) were purchased from Model Animal Research Center, Nanjing University (Nanjing, China). Animals were raised in Southern Medical University in specific-pathogen-free animal rooms, maintained at 22 °C with a 12 h light/dark cycle with free access to chow and drinking water. All the experimental procedures using mice were approved by the Institutional Animal Care and Use Committee of Southern Medical University and were conducted in accordance with institutionally approved protocols and guidelines for animal care and use.

2.2. *Isolation of mouse peritoneal macrophages and cells culturing*

Thioglycollate-elicited macrophages were recovered 3 days after i.p. injection of 3 mL thioglycollate medium (brewer modified; 3% *w/v*), by collecting the peritoneal lavage using 30 mL of PBS. The peritoneal macrophages were cultured in RPMI cell culture medium for 2 h. After adherence, cells were washed and cultured in fresh RPMI medium [RPMI containing 10% heated FBS, 1% penicillin and streptomycin] for 24 h before used in the experiments. RAW 264.7 macrophages, Human PBMCs and THP-1 were cultured in RPMI cell culture medium (RPMI containing 10% FBS, 1% penicillin and streptomycin). THP-1 differentiated macrophages were collected by treatment with PMA (100 nmol/L) for 24 h, and cells were washed with PBS and cultured with fresh RPMI medium for 24 h before used. HEK-Blue hTLR2 cells, HEK-Blue hTLR3 cells, HEK-Blue hTLR4 cells, HEK-Blue hTLR7 cells, HEK-Blue hTLR8 cells, HEK-Blue Null cells and A549 cells were cultured in DMEM cell culture medium (DMEM containing 10% FBS, 1% penicillin and streptomycin). All cells were incubated at 37 °C in a 5% CO_2 humidified incubator.

2.3. *Secreted alkaline phosphatase (SEAP) reporter assay*

HEK-Blue hTLR cells lines were seeded in 384-well plate (4×10^4 cells per well) with 20 μL DMEM medium (containing 10% heat-inactivated FBS), and cultured with 20 μL of DMEM medium containing indicated concentrations compounds with or without TLR-specific agonists at 37 °C in a 5% CO_2 humidified incubator for 24 h. After incubation, another 40 μL of Quanti-Blue solution (req-qb12, Invivogen) was added and incubated for 30 min. Absorbance was measured at 620 nm using a microplate reader. The IC_{50} of compound was calculated and processed using Origin 9.0 software. TLR-specific agonists to selectively activate respective TLRs: Poly I:C, lipopolysaccharide (100 ng/mL, tlrl-b5lps, Invivogen), Pam_3CSK_4 (200 ng/mL, tlrl-pms, Invivogen), Pam_2CSK_4 (200 ng/mL, tlrl-pm2s-1Invivogen) and R848 (5 μg/mL, tlrl-r848, Invivogen) were used. Value of IC_{50} were calculated and fitted using Origin 9.0 software.

2.4. *In vivo anti-atherosclerosis study of SMU-CX24*

To generate atherosclerosis mouse model, 8-weeks old $ApoE^{-/-}$ mice were fed with a Western diet containing 1.25% cholesterol and 20% fat (Jiangsu Xietong Pharmaceutical Bioengineering) for 12 weeks. Mice were treated s.c. with SMU-CX24 (5 mg/kg dissolved in citrate-disodium phosphate buffer, pH = 7.0) or vehicle control (buffer alone), and weighed on alternate days for the last 8 weeks. Mice were sacrificed by cervical dislocation under anesthesia. Serum samples were obtained from orbital blood by centrifuging at 7000 rpm, and total cholesterol (A111-1-1, TBD Science), triglyceride (A110-1-1, TBD Science), LDL-C (A113-1-1, TBD Science), and cytokine IL6 and CCL5 were detected according to manufacturer's instructions. Tissues were isolated, fixed in 4% paraformaldehyde for staining or snap frozen for further biology experiments. For atherosclerotic lesion analysis, *in-situ* aorta tissues without perivascular connective tissues were prepared, then fixed in black wax Petri dish and stained with Oil Red O. Heart and liver tissues were embedded in tissue-Tek OCT compound (4583, SAKURA), and 6 μm slices were sectioned using Leica cryostat (CM1950, Leica) for Oil Red O staining. Paraffin-embedded heart tissues were also prepared, and indicated to standard H&E, MASSON, immunohistochemical staining and immunofluorescence analyses. The following primary antibody specific for rabbit-TLR3 (1:600, ab137722, Abcam), mouse α-SMA antibody (1:6000, ab7817, Abcam) and rabbit F4/80 antibody (1:500, 70076, Cell Signaling). All the sections were examined under Zeiss Axiovert 200M microscope using AxioVision software. Both lesion area and total area were measured with image J software to relatively quantify. For Western blot, the whole tissues lysates extracted from frozen aorta and liver tissues by RIPA buffer (with protease inhibitor, phosphatase inhibitor and PMSF) and ultrasonication, was indicated to analysis of TLR3 expression with primary anti-rabbit TLR3 antibody. For RT-PCR, total RNA extracted from frozen aorta and liver tissues were collected and used for indicated gene expression of *TNFα*, *IL6*, *IL1β*, *INOS*, *Vcam-1*, *Ccl5* and *Mmp2*.

2.5. *Synthesis of compounds and their structural characterization*

The procedure for synthesis and structural characterization of 9-methoxy-elliciptine (CX1), SMU-CX24 and its derivatives are provided in the Supporting Information Notes S1 and S2.

2.6. *Statistical analysis*

Data are expressed as mean ± standard deviation (SD). Statistical analysis was done using an unpaired two-tailed Student's *t* test.

*$P < 0.05$; **$P < 0.01$; ***$P < 0.001$ and ns denotes not significant. Value of $P < 0.05$ was considered as statistically significant. Other experimental materials and methods are included in the Supporting Information.

3. Results

3.1. *TLR3 was involved in atherosclerosis regulation*

Atherosclerosis is driven by multiple factors but the role of TLR3 expression in this process remains unclear. To explore the potential role of TLR3 in atherosclerosis, we first ascertained the presence of TLR3 expression in sections of human artery with atherosclerotic plaques from atherosclerotic patients and determined whether TLR3 were associated with atherosclerosis injury. Atherosclerosis is characterized by foam cell accumulation in atherosclerotic plaque lesions, and macrophages engulf oxidized lipid particles and thereby develop into to foam cells. Specimens were indicated to H&E staining for the pathologically analysis (Fig. 1A) and immunofluorescence staining of cross-sectioned atherosclerotic specimens stained with antibodies against TLR3 and CD68. We observed that TLR3 protein localizes to CD68-positive macrophages within plaque lesion, suggesting that lesion plaque macrophages expressed TLR3 and TLR3 was involved in macrophages mediated atherosclerosis regulation (Fig. 1B, top). During atherosclerosis pathologically condition, multiple factors affected the phenotypic change of vascular smooth muscle (VSMC) and endothelial cells (EC) injury within lesion in the intima. We observed that TLR3 also were contributed to VSMC modification and EC injury, and TLR3 localizes to CD31-positive EC and α-SMA-positive VSMC within denatured intima (Fig. 1B, middle and bottom). Theses evidenced indicated that aberrant expression of TLR3 within atherosclerotic lesion cells type and TLR3 involved in the human atherosclerosis process.

Subsequently, we carried out RNA-seq bioinformatics analysis and RT-PCR confirmation in PBMCs from patients with severe atherosclerosis symptoms and asymptomatic healthy donors (Fig. 1C). After RNA-seq analysis, there are 470 significant genes expression upregulated (fold change >2 and P value < 0.05) and 355 downregulated (fold change <0.5 and P value < 0.05) in atherosclerotic patients ($n = 4$) *versus* healthy individuals ($n = 3$) (Supporting Information Fig. S1A). We found that differentially expressed genes were significantly enriched among immune response and virus defense categories by functional KEGG analysis, and the TLR signaling pathway was involved ($P < 0.05$, Fig. S1B). Further investigation in proving TLR3 expression and atherosclerosis using PBMCs from 18 patients and 11 healthy individuals was conducted. Similar results were obtained significantly higher TLR3 expression was observed in patient specimens than in healthy controls (Fig. 1C). These data indicated that TLR3 was involved in atherogenesis and the inflammatory response in human atherosclerosis progression, and we proposed that an effective intervention in TLR3 expression might alleviate atherosclerosis.

We further used oxidized low intensity lipoprotein (oxLDL) as a substrate to induce foam cell formation in macrophages and mimic the events in atherosclerotic lesions, to explore whether TLR3 deficiency could affect macrophage-mediated foam cell formation. As expected, silencing *TLR3* in macrophages markedly decreased the oxLDL induced foam cell formation (Fig. 1D), which indicated that TLR3 regulated foam cell formation in macrophages and silencing *TLR3* inhibited this process. The silencing efficacy of TLR3 siRNA treated peritoneal macrophages was shown in Fig. S1C. These results implied that TLR3 was an atherogenic factor and inhibiting TLR3 could be strategy for treating atherosclerosis. However, the lack of specific TLR3 inhibitors precluded the evaluation of pharmacological intervention strategies of TLR3 expression for treating atherosclerosis.

Although several TLR3 inhibitors have been identified, their activity and specificity need to be improved substantially for various reasons. First, complicated protein-RNA interactions are essential for the recognition of dsRNA by TLR3, which needs to homodimerize to initiate immune responses[29,30]. Second, the presence of several (10 human and 12 murine) homologous TLRs sharing a double horseshoe-shaped ligand binding domain[31], makes it very difficult to synthesize specific TLR3 inhibitors. Finally, the commercially available TLR3 agonist poly I:C was also reported to elicit inflammatory responses *via* retinoic acid inducible gene-1 (RIG-1) and melanoma differentiation-associated protein 5 (MDA5) receptors[32]. Based on this evidence, we hypothesized that pharmacological disruption of TLR3 may be a novel way to treat atherosclerosis. Hence, the identification, synthesis and evaluation of specific TLR3 inhibitors with significant efficacy and specificity were the first steps in developing new therapeutics against atherosclerosis.

3.2. *Discovery of a novel TLR3 inhibitor*

To develop novel specific TLR3 inhibitors, we identified potent hits by cell-based high throughput screening (HTS) using a small-molecule library containing 15,700 compounds (Maybridge and NCI) with nitric oxide (NO) as an indicator in RAW 264.7 macrophages (Fig. 2A). Briefly, exposure to Poly I:C, a synthetic long double-stranded RNA analog, selectively activated TLR3 and led to significant NO production. For the first time, we identified NSC69187 (9-methyoxy-elliciptine, named CX1) as the most potent hit among those with favorable TLR3 inhibitory activity (Supporting Information Fig. S2). Since Poly I:C also stimulates the MDA-5 and RIG-1 signaling pathways and subsequent inflammation, we next used HEK-Blue hTLR3 cells, which is a cell line that is stably transfected with human TLR3, which expresses a secreted alkaline phosphatase (SEAP) reporter gene after TLR3 activation. Our data further verified that CX1 inhibited TLR3 with an IC_{50} value of 0.12 ± 0.01 μmol/L, as determined by SEAP assay (Fig. 2B). CX1, a natural alkaloid derived from *Ochrosia elliptica*, was recognized as a broad-spectrum antitumor drug with significant cell cycle and topoisomerase II inhibitory activities[33,34]. However, the lack of aqueous solubility and significant biotoxicity precluded its clinical application. To synthesize a more potent TLR3 specific inhibitor with structural novelty and bioavailability, we performed several chemical optimizations based on the structure of CX1. First, we synthesized CX1 as previously reported[35]. Next, we developed several concise synthetic routes based on CX1 to achieve a series of potent TLR3 inhibitors, which allowed an extensive structure−activity relationship (SAR) analysis (for representative syntheses and compound characterizations, see Note S1 and Note S2; for SAR results, see Supporting Information Table S1). Briefly, we first substituted the $-OCH_3$ group at the 9th position of CX1 with electron withdrawing or electron donating groups of different sizes. As shown in our data, the introduction of electron-donating but not electron-withdrawing groups notably increased TLR3 inhibitory activity. In addition, groups with weak alkaline properties enhanced TLR3 inhibitory activity irrespective of the size of the substituent. Second, after keeping the -OCH_3 group in CX1, *N*-

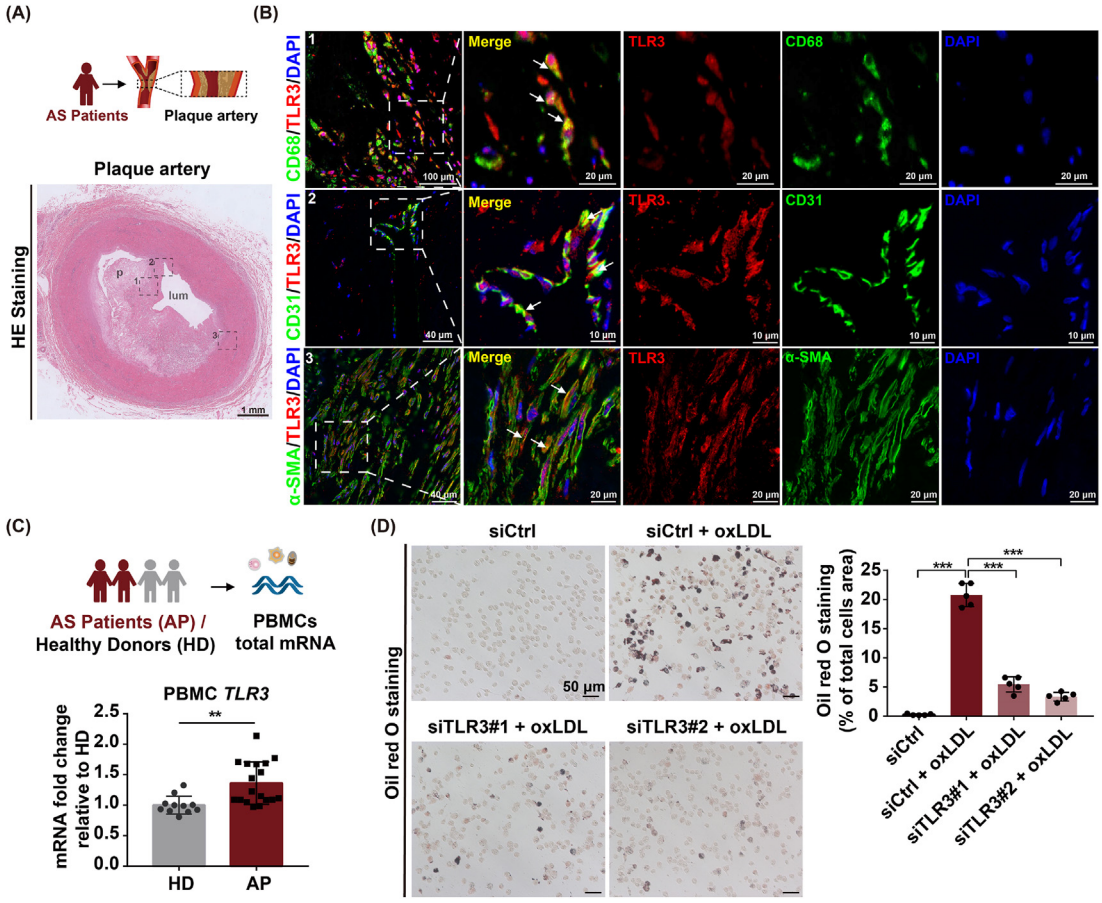

Figure 1 TLR3 is involved in atherosclerosis regulation. (A) Schematic illustration of plaque artery sections isolated from arteriosclerotic patients (top) and histological cross-sections of plaque artery were subjected to H&E staining (bottom). (B) Representative immunofluorescence staining of TLR3 (red), macrophage marker CD68 (green, top), endothelial cells CD31 marker (green, middle), smooth muscle cell marker α-SMA (green, bottom) and counterstained with DAPI (blue). Enlargement of the insert shown colocalized pixels and white arrows indicated co-location of TLR3 and CD31, CD68, or α-SMA ($n = 3$). (C) Schematic illustration of PBMCs collected from atherosclerosis patients and asymptomatic healthy donors. RT-qPCR analysis of PBMC specimens from atherosclerosis patients ($n = 18$) and asymptomatic healthy adults ($n = 11$) indicated significant gene expression of *TLR3* in atherosclerosis patients. (D) Primary peritoneal macrophages transfected with 20 nmol/L negative control siRNA (siCtrl) or 20 nmol/L TLR3 siRNA (siTLR3#1 and siTLR3#2) were challenged with 50 μg/mL oxLDL for 24 h. Representative images and quantitative analysis of treated cells stained with oil red O were shown ($n = 5$). Data are expressed as the mean ± SD. Statistical significance was determined using unpaired two-tailed Student's *t* test. $^*P < 0.05$; $^{**}P < 0.01$; $^{***}P < 0.001$ *versus* healthy donors, or control incubated with oxLDL. AS, atherosclerosis; p, plaque; lum, lumen.

alkylated or *N*-alkylated quaternary compounds were synthesized in the position of indole and isoquinoline, which exhibited poor TLR3 inhibitory activity compared to the parent compound (CXI), suggesting the indispensable nature of indole and isoquinoline structures in potency and affinity to TLR3. Ultimately, we identified compound SMU-CX24, with a $-CH_2NHCH(CH_3)_2$ substitute at the 9th position of ellipticine (Fig. 2A and Supporting Information Fig. S3), which exhibited significant TLR3 specific inhibition with an IC_{50} value of 18.87 ± 2.21 nmol/L, an improvement of approximately ten-fold compared to that of the parent compound CX1 (Fig. 2B). In addition, a major challenge in developing natural products as drugs involves solubility, which in turn affects bioavailability. As shown in Fig. 2C, the optimized compound (SMU-CX24) was completely soluble in citrate sodium phosphate buffer (0.1 mol/L, pH = 7.0), showing better aqueous solubility properties than CX1, and maintaining its TLR3 inhibitory activity as previously described (Supporting Information Fig. S4).

In addition to efficacy, specificity is also a significant attribute of TLR inhibitors. We therefore examined SMU-CX24 against a panel of homologous TLRs (TLR1/TLR2, TLR2/TLR6, TLR3, TLR4, TLR7 and TLR8) using TLR-specific ligands to activate specific TLR-mediated SEAP production in HEK-Blue hTLR cells. We observed specific inhibition of TLR3 signaling by SMU-CX24 in intact cells but not by homologous TLRs (Fig. 2D). Thus, we here identified the first reported TLR3-specific inhibitor, SMU-CX24, which has high efficacy, aqueous solubility and TLR3 specificity. Given the favorable inhibition of TLR3 by SMU-CX24, we next explored its physical properties, mechanistic bioactivity and anti-atherosclerotic effect.

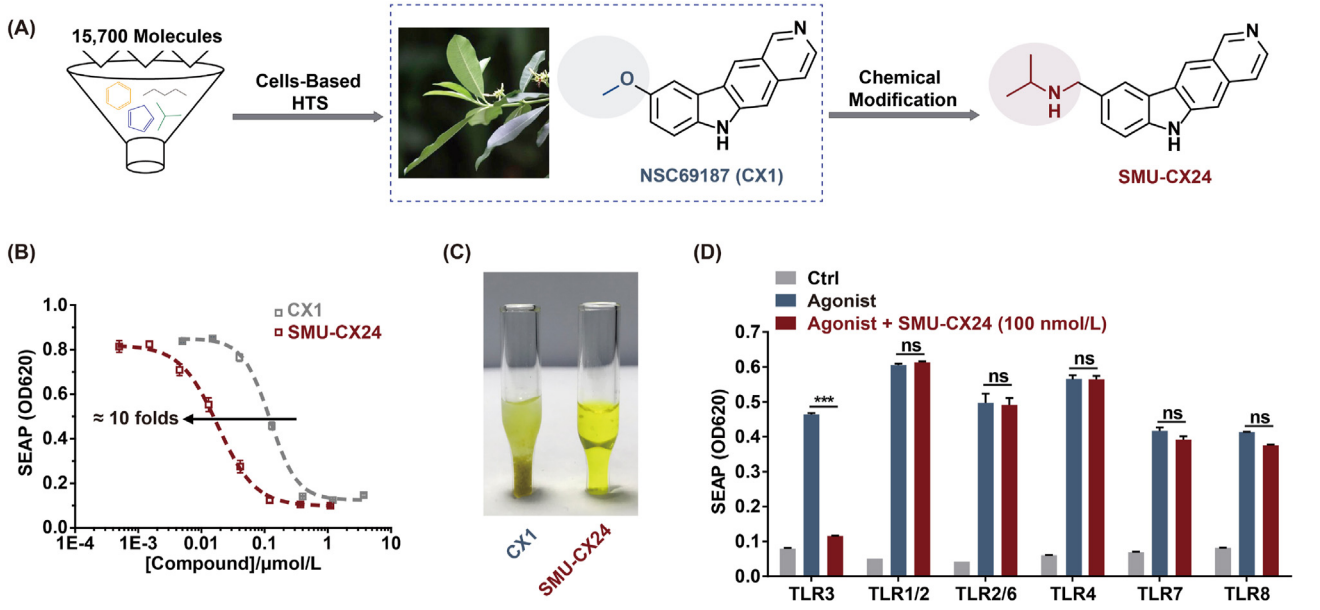

Figure 2 SMU-CX24 inhibited TLR3 with significant potency and specificity. (A) Schematic illustration of NSC69187 (CX1) discovery and the subsequent modifications performed to synthesize SMU-CX24. (B) Dose-dependent inhibition of Poly I:C (10 μg/mL) elicited SEAP signaling in HEK-Blue hTLR3 cells at the indicated concentrations of CX1 and SMU-CX24. SMU-CX24 inhibited TLR3-mediated SEAP signaling with an IC_{50} of 18.87 ± 2.21 nmol/L, which showed approximately a tenfold inhibitory activity against TLR3 compared to the parent compound, CX1. (C) Visual appearance of SMU-CX24 and CX1 (40 mmol/L) dissolved in sodium citrate phosphate buffer (pH = 7.0). SMU-CX24 but not CX1 was absolutely dissolved. (D) Specificity test for SMU-CX24 (100 nmol/L) with different TLR-specific agonists in HEK-Blue hTLR cells that overexpressed TLRs, and SMU-CX24 selectively inhibited TLR3-activated SEAP signals but not that of other homologous TLRs. TLR-specific agonists were used to selectively activate TLRs: 100 ng/mL lipopolysaccharide (TLR4), 200 ng/mL Pam_3CSK_4 (TLR1/2), 200 ng/mL Pam_2CSK_4 (TLR2/6) and 5 μg/mL R848 (TLR7 and TLR8). Data in (B, D) are expressed as the mean ± SD. of three independent experiments. Statistical significance was determined using unpaired two-tailed Student's *t* test. $^*P < 0.05$; $^{**}P < 0.01$; $^{***}P < 0.001$ and ns denotes not significant *versus* control incubated with Poly I:C or positive control.

3.3. *SMU-CX24 exhibited unexpected fluorescence properties and TLR3 affinity*

Due to its complex conjugated structure, we hypothesized that SMU-CX24 possessed fluorescence properties. Consistently, we observed a significant fluorescence signal from SMU-CX24 with maximal excitation at 399 nm and emission at 521 nm (Fig. 3A). Next, we considered whether SMU-CX24 could attract and attach to cells to mediate the inhibition of TLR3. Therefore, peritoneal macrophages and RAW 264.7 macrophages co-cultured with the indicated concentration of SMU-CX24. The results showed that a dramatic increase in fluorescence intensity was detected by flow cytometry and microscopy, which indicated the binding of SMU-CX24 to peritoneal macrophages (Fig. 3B and C) and RAW 264.7 cells (Supporting Information Fig. S5A and B) in a concentration-dependent manner. These data demonstrated the capacity of SMU-CX24 to attach to the cell and achieve TLR3 inhibition. Thus, we further explored the binding mode of SMU-CX24 to TLR3 protein in a molecule-protein interaction model.

To quantitatively evaluate the ligand-binding affinity of SMU-CX24 for TLR3, we first investigated the binding affinity of SMU-CX24 for purified recombinant TLR3 using surface plasmon resonance (SPR) analysis, by determining the dissociation constant (K_D). Briefly, serial dilutions of SMU-CX24 (6.25−50 μmol/L) were injected into the flow system and bound to immobilized TLR3 in a 3D dextran sensor chip. Data analysis of the binding curve fitting yielded the ligand-binding affinity of SMU-CX24 with a K_D of 22.0 nmol/L (Fig. 3D), and a moderate association rate constant (k_a = 457 L/mol·s) and dissociation rate constant (k_d = 0.0101 ms^{-1}). We further explored the ligand-binding affinity of SMU-CX24 to TLR3 using a fluorescence method in which we titrated indicated concentrations of SMU-CX24 (5−20.48 nmol/L) with TLR3 protein (0.1 μmol/L), and an extrinsic fluorescence probe coupled to the TLR3 protein was excited at 280 nm and emitted at 399 nm. As shown in Fig. S6A, SMU-CX24 bound to TLR3 protein in a concentration-dependent manner with a K_D value of 15.87 ± 2.21 nmol/L (Supporting Information Fig. S6A), while the ligand-binding activity of the negative control (CX1-b) was negligible (Fig. S6B). Similar binding constants (K_D) were determined in the different models (SPR and fluorescence), confirming the high binding affinity of SMU-CX24 to TLR3, which was similar to inhibition of TLR3 in HEK-hTLR3 cells.

Next, we considered whether SMU-CX24 was capable of competing with Poly I:C to bind to TLR3. Thus, we examined the effect of SMU-CX24 on rhodamine-labeled Poly I:C uptake by peritoneal macrophages. After cells were exposed to SMU-CX24 (1 μmol/L), a modest reduction in rhodamine intensity within the cells was observed, indicating the inhibitory effect of SMU-CX24 on Poly I:C intake (Fig. 3E). Therefore, to a certain extent, SMU-CX24 might share the same binding site with Poly I:C for TLR3 at the cellular level and affect the dissociation of the TLR3-dsRNA complex. To further confirm this hypothesis, we conducted a replacement assay using rhodamine-labeled Poly I:C as a probe to bind to the TLR3 protein with the subsequent addition of the indicated concentrations of SMU-CX24. Extrinsic fluorescence of rhodamine-labeled Poly I:C was

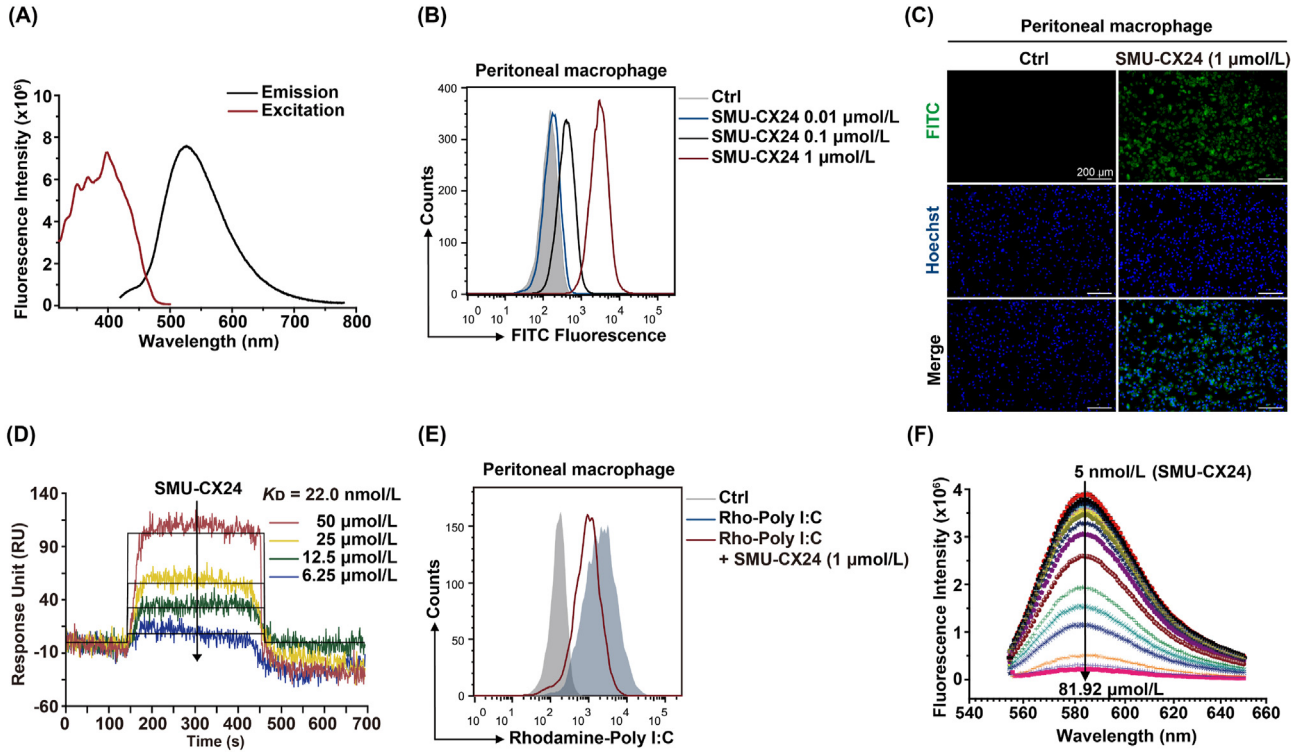

Figure 3 SMU-CX24 inhibited TLR3 with high affinity. (A) SMU-CX24 (1 μmol/L) has notable fluorescence intensity with a maximal excitation at 399 nm and emission at 521 nm. (B) and (C) Peritoneal macrophages were incubated with SMU-CX24 (0, 0.01, 0.1 and 1 μmol/L) for 4 h and cellular fluorescence were analyzed by (B) flow cytometry and (C) fluorescence microscope (Green: SMU-CX24; Blue: nuclei; Scale bars represent 200 μm). (D) Binding curves of SPR analysis of the indicated concentrations of SMU-CX24 (varying from 6.25 to 50 μmol/L) and TLR3. Data fitting to a Langmuir binding model gave a K_D value of 22.0 nmol/L. (E) Flow cytometry analysis of peritoneal macrophages treated with rhodamine-labeled Poly I:C (1 μg/mL) for 4 h with or without SMU-CX24 (1 μmol/L) incubation. (F) SMU-CX24 competed rhodamine-labeled Poly I:C to bind with TLR3. Rhodamine-labeled Poly I:C (1 μg/mL) was incubated with TLR3 (0.05 μmol/L), and then the indicated concentrations of SMU-CX24 (5−81.92 nmol/L) were added. The extrinsic fluorescence of rhodamine-labeled Poly I:C was excited at 546 nm, and an emission at 555−650 nm was recorded.

excited at 546 nm, and an emission at 555−650 nm was recorded. As shown in Fig. 3F, SMU-CX24 significantly reduced rhodamine-labeled Poly I:C fluorescence in a concentration-dependent manner, while the negative control CX1-b was negligible in competing with Poly I:C for binding to TLR3 (Fig. S6C). These data demonstrated that SMU-CX24 was a competitive inhibitor of Poly I:C that bound to the TLR3 heterodimer with high affinity, which further verifies that SMU-CX24 inhibited TLR3.

3.4. Remarkable effects of SMU-CX24 against TLR3-activated inflammatory responses

Based on these data, we next studied the mechanistic role of SMU-CX24 in the TLR3 signaling cascade. We first explored the effects of SMU-CX24 on Poly I:C-induced TLR3 expression in mouse peritoneal macrophages. As demonstrated, Poly I:C upregulated *TLR3* gene expression, and SMU-CX24 inhibited TLR3 expression in a dose-dependent manner (Fig. 4A). However, at the in translated level, no significant TLR3 expression was induced by Poly I:C exposure for the indicated times in peritoneal macrophages or HEK-Blue hTLR3 cells (Supporting Information Fig. S7A and B). We further investigated the role of SMU-CX24 in HEK-Blue hTLR3 and A549 cells that overexpressed TLR3, and the data showed that TLR3 expression was almost completely abolished in both cell lines in response to 5 μmol/L SMU-CX24 (Fig. S7C and D). Next, the effect of SMU-CX24 on TLR3-induced intracellular signal-regulated proteins was also explored. SMU-CX24 also reversed Poly I:C regulated the level of phosphorylated P65, P38, ERK and TBK-1 and IκBα expression in whole cell lysates of peritoneal macrophages (Fig. 4B−D and Fig. S7E−I). Further, to explore the inhibitory effects of SMU-CX24 on TLR3 activated production of proinflammatory cytokines, primary peritoneal macrophages, human peripheral blood mononuclear cells (PBMCs) and cultured RAW 264.7 macrophages were used. After treatment with SMU-CX24, the gene expression of *IFNα* and *IFNβ* induced by Poly I:C was significantly inhibited (Fig. 4E and F), and significantly better than the available commercial TLR3 inhibitor CU-CPT 4a (Supporting Information Fig. S8). The production of NO and IL-6 in the supernatant of Poly I:C-induced peritoneal macrophages (Fig. 4H and I), TNF-α in RAW 264.7 cells, and TNF-α and IL-1β in human PBMCs (Fig. 4J and K) were also reduced by SMU-CX24 treatment. *In vivo*, C57BL/6J mice were pretreated with the indicated concentrations of CX24 and subsequently exposed to Poly I:C (250 μg/kg) for 4 h. Poly I:C-induced

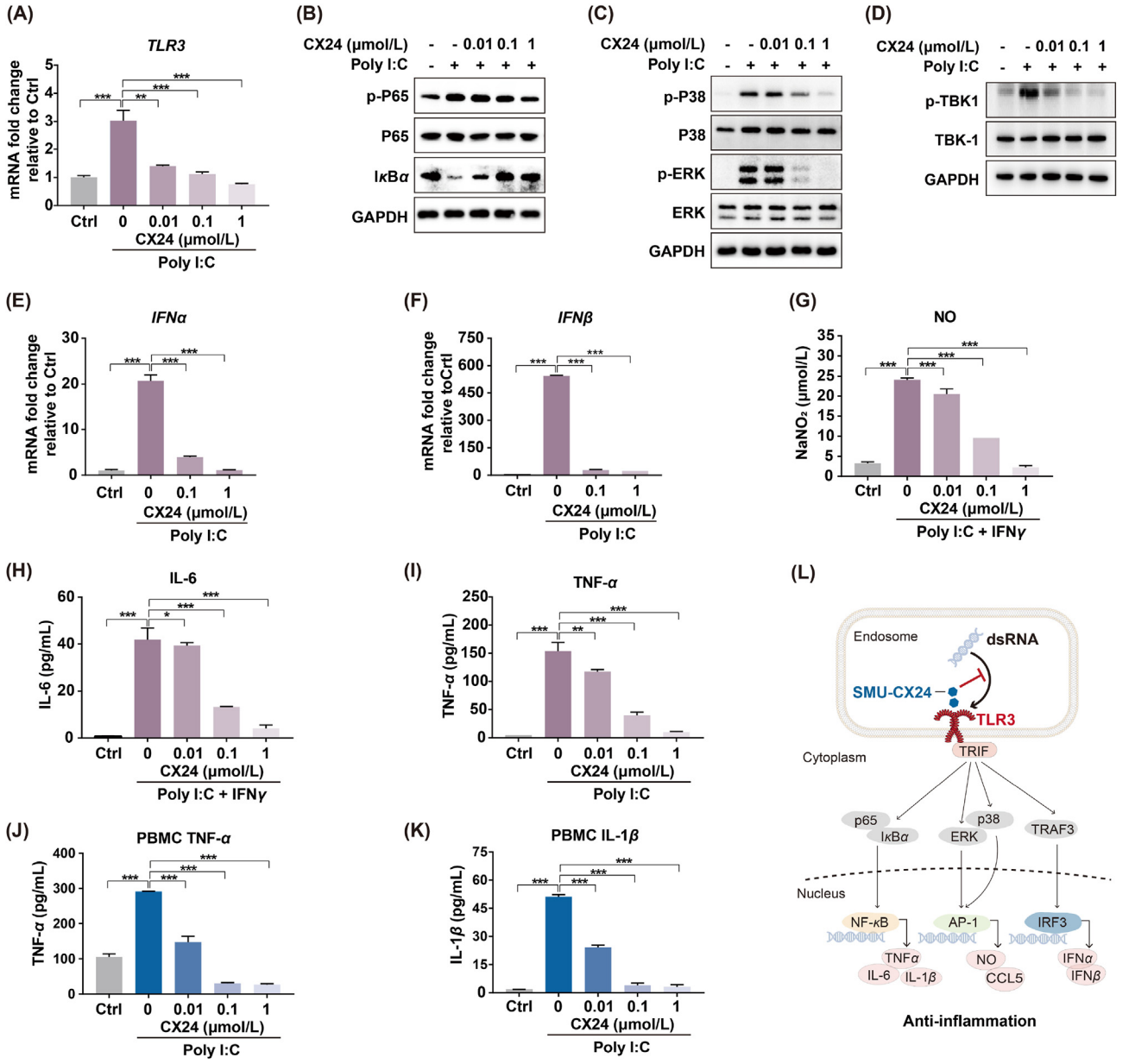

Figure 4 SMU-CX24 inhibited TLR3-activated signaling cascades and subsequent inflammatory responses. (A) Peritoneal macrophages were pretreated with indicated concentration of SMU-CX24 (0.01, 0.1 and 1 μmol/L) and subjected to Poly I:C (10 μg/mL) exposure for 4 h. Representative *TLR3* gene expression of treated cells were analyzed. (B−D) Peritoneal macrophages were pretreated with indicated concentration of SMU-CX24 (0.01, 0.1 and 1 μmol/L) and subjected to Poly I:C (10 μg/mL) exposure for 1 h. Protein expression of phosphorylated or total of P65, P38, ERK, TBK-1 and IκBα were analyzed. (E) and (F) Peritoneal macrophages were pretreated with indicated concentration of SMU-CX24 (0.01, 0.1 and 1 μmol/L) and subjected to Poly I:C (10 μg/mL) exposure for 12 h. Representative *IFNα* and *IFNβ* gene expression of treated cells were analyzed. (G−K) TLR3-induced expression of inflammatory factors was inhibited by SMU-CX24 in both primary and cultured cell lines. NO (G) and IL-6 (H) in the supernatant of Poly I:C-induced peritoneal macrophages for 48 h, TNF-α in RAW 264.7 cells for 24 h (I), TNF-α (J) and IL-1β (K) human in PBMC for 24 h, were dose-dependently inhibited by SMU-CX24 (0, 0.01, 0.1 and 1 μmol/L). (L) Schematic illustration showing that SMU-CX24 decreased TLR3-induced NF-κB, MAPK and IFN signaling pathways and inflammatory responses. The Data are expressed as mean ± SD. of three independent experiments. Statistical significance was determined using unpaired two-tailed Student's *t* test. $^{*}P < 0.05$; $^{**}P < 0.01$; $^{***}P < 0.001$ *versus* control incubated with Poly I:C.

plasma CCL5 expression was also greatly inhibited by SMU-CX24 (Supporting Information Fig. S9). Collectively, these data demonstrated that SMU-CX24 also exerted an inhibitory effect on TLR3-activated NF-κB, MAPK and IFN signaling pathways and inflammatory responses, as shown in Fig. 4L.

3.5. *Notable efficacy of SMU-CX24 against atherogenic factors and foam cell formation*

Due to the lack of TLR3 inhibitors with high efficacy and specificity, pharmacological intervention to explore the protective

effect of TLR3 deficiency in atherosclerosis has been precluded. Herein, substantial evidence that indicated SMU-CX24 had notable TLR3 specificity and anti-inflammatory effects. To preliminarily investigate the potential therapeutic role of SMU-CX24 on atherosclerosis, C57BL/6J mice were pretreated with a subcutaneous injection of SMU-CX24 (5 mg/kg), and then treated with vehicle or 12.5 mg/kg Poly I:C by s.c. injection for 24 h. None of the treated mice showed any apparent adverse effects. Total RNA was isolated from the aortic tissues of treated mice for analysis, and the experimental procedure was shown in Fig. 5A. SMU-CX24 significantly decreased the Poly I:C-induced expression of *TLR3* in aortic tissues. In the initial stage of atherogenesis, circulating monocytes are recruited and differentiated into monocyte-macrophages in vascular endothelial cells in response to atherogenic cytokines including chemokines and adhesion molecules produced by the complex environment. Monocyte-macrophages uptake oxLDL and form foam cell[36,37]. In parallel, the effect of SMU-CX24 on primary pro-atherosclerotic chemokines and adhesion molecules associated with atherogenesis was also investigated. We observed that gene expression of TLR3-induced *Vcam-1*, *Icam-1*, *Ccl2* and *Ccl5* in the aorta tissues was significantly inhibited after treatment with SMU-CX24 (Fig. 5A), suggesting the effect of SMU-CX24 on the pro-atherosclerotic cytokine expression. In addition, we established an *in vitro* oxLDL-induced foam cell model in peritoneal macrophages and examined whether SMU-CX24 could inhibit foam cell formation. As expected, SMU-CX24 treatment significantly inhibited oxLDL-induced foam cell formation in macrophages in a dose dependent manner (Fig. 5B). We further explored the role of SMU-CX24 on the oxLDL uptake in macrophages. Cellular fluorescence results shown that SMU-CX24 treated macrophages notably reduced oxLDL uptake and perhaps benefited to inhibit foam cells formation (Fig. 5C and D). In addition, SMU-CX24 treatment also mediated inflammatory response inhibition by reducing the oxLDL induced inflammatory cytokine *IL-6* and *IL-1β* expression to exert the anti-atherosclerosis effect (Fig. 5E), but not cholesterol efflux related gene *Abca1* and *Abcg1* expression (Fig. 5F). In general, SMU-CX24 preformed a notable inhibitory effect on TLR3-induced pro-atherosclerotic chemokine, adhesion molecules production and oxLDL-induced foam cell formation, exhibiting promising therapeutic potential for atherosclerosis treatment.

3.6. *Promising therapeutic effects of SMU-CX24 on atherosclerosis*

Based on the notably effect of SMU-CX24 on inhibiting atherogenic cytokines productions, as well as foam cell formation, its anti-atherosclerotic effects were then evaluated in depth using a standard atherosclerotic mouse model. Briefly, ApoE$^{-/-}$ mice were fed with a Western diet (1.25% cholesterol and 20% fat) for up to 12 weeks and concomitantly treated with SMU-CX24 (5 mg/kg) or vehicle every other day during the last 8 weeks (Fig. 6A). The mice were then euthanized and histological analysis was performed with respect to examine lesion composition of lipids, collagen, smooth vasculature and inflammatory responses. Compared to that in the vehicle control, Oil O red staining shown less of aortic plaques in the lesion areas of both the en face *in-situ* aorta and aortic root harvested from SMU-CX24-treated animals (Fig. 6B), and SMU-CX24 treatment also induced a more than 50% reduction in the necrotic area (Fig. 6C, H&E staining, dotted line). These data indicated SMU-CX24 treatment reduced lesion area and exhibited notable anti-atherosclerosis effect. In addition, plaque collagen content (Masson staining) was significant expressed in aortic root from mice with SMU-CX24 exposure (Fig. 6D), accompanying with reduced α-SMA positive cells accumulation within plaque area, perhaps suggesting that SMU-CX24 treatment reduced the lesion vascular smooth muscle cells (VSMCs, α-SMA staining) migration from the media to the intima and the subsequent modification (Fig. 6D), which benefited to collagen degradation inhibition and plaque stability with atheroprotective effect. On the other hand, serum lipid levels, including LDL-C, TG and T-CHO, showed significant reduction after SMU-CX24 treatment (Fig. 6E). Even after 12 weeks of treatment, no significant body weight changes, or histologic changes in the kidney and liver were observed (Supporting Information Fig. S10). Collectively, these data indicated that SMU-CX24 alleviated atherosclerosis by reducing atherogenic burden and increasing atherosclerotic protection.

To further evaluate the intrinsic mechanism of SMU-CX24 and whether TLR3 mediated inflammatory regulation involved in atherosclerosis process, we next analyzed the aortic inflammation expression of the treated mice. Herein, a significant reduction of aortic TLR3 expression were observed in SMU-CX24 treated mice compared with vehicle control at both transcription and translation level (Fig. 7A), suggesting that SMU-CX24 mediating TLR3 inhibition involving in the atherosclerosis regulation. In addition, gene analysis revealed that aorta from SMU-CX24 treated mice exhibited a notable reduction in inflammatory cytokines expression including *TNFα*, *IL1β* and *IL6* (Fig. 7B), which contributed to alleviated inflammation infiltration within atherosclerotic lesion. Atherosclerotic inflammatory responses regulated the lesion environment and influenced the pathological development, including further lesion formation, plaque stability, and VSMC proliferation and migration. Consistently, a significant reduction in inflamed cells secreted *Ccl5*, *Vcam-1*, matrix metalloproteinase 2 (*Mmp2*) was observed in the aorta of the SMU-CX24 treated mice (Fig. 7C). In addition, SMU-CX24 treatment also significantly reduced the serum IL6 and CCL5, exhibiting notable anti-inflammatory effect (Fig. 7D). These data indicated that SMU-CX24 treatment reduced lesion inflammation and contributed to inhibit atherosclerosis development. Under atherosclerosis pathological conditions, macrophages play vital roles in both inflammatory response and cholesterol efflux. We observed F4/80 positive cells within aortic root were notably decreased from mice after SMU-CX24 exposure (Fig. 7E). The expression proinflammatory cytokines *INOS*, a M1 macrophage marker, were also decreased in aorta tissue from SMU-CX24 treated mice (Fig. 7E), indicating that SMU-CX24 mediated inflammation inhibition perhaps regulated the macrophages infiltration within atherosclerotic lesion, which benefited to foam cells formation and atherosclerosis alleviation. However, no major differences were observed in the expression of the macrophage-modulated cholesterol efflux by liver X receptor-dependent genes in the aorta after SMU-CX24 treatment, including *Lxrα*, *Lxrβ*, *Abca1*, *Abcg1*, *Srebp1* and *Srebp2* (Fig. 7G). Previous studies have also revealed the role of TLR3 activation in liver lipid metabolism disorder[16,24]. Herein, a reduction in the liver lipid levels in SMU-CX24 treated mice was observed after SMU-CX24 exposure (Fig. 7H), accompanied with a notable reduction in TLR3 expression in SMU-

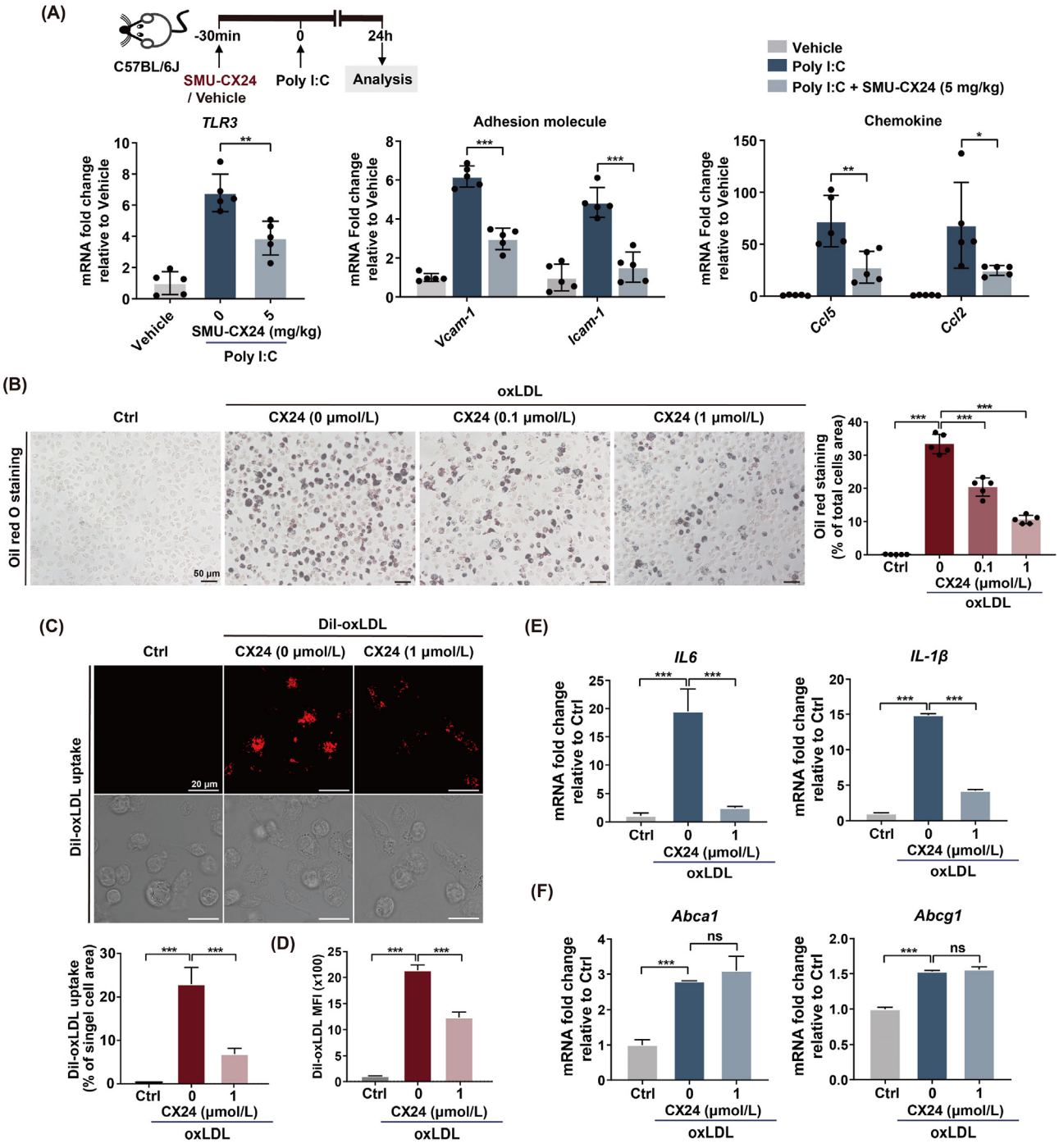

Figure 5 Notable effect of SMU-CX24 against atherogenic factors and foam cell formation. (A) The experimental procedure indicated that C57BL6/J mice were pretreated with the indicated doses of SMU-CX24 (0, 0.5, 5 or 50 mg/kg) dissolved in disodium hydrogen phosphate citrate buffer (pH = 7.0) for 30 min prior to Poly I:C (12.5 mg/kg) injection for 24 h. Gene expression of *TLR3, Vcam-1*, *Icam-1*, *Ccl2* and *Ccl5* of aorta isolated from treated mice were analyzed ($n = 5$ per group). (B) Peritoneal macrophages were pretreated with indicated concentration of SMU-CX24 (0.1 and 1 μmol/L) and subjected to oxLDL (50 μg/mL) exposure for 24 h. Representative images and quantitative analysis of Oil red O staining of treated cells were shown. (C) and (D) Peritoneal macrophages were pretreated with indicated concentration of SMU-CX24 (0.1 and 1 μmol/L) and subjected to Dil-oxLDL (10 μg/mL) exposure for 4 h. (C) Representative confocal images and quantitative analysis of cellular Dil-oxLDL uptake, and (D) the mean fluorescence intensity (MFI) analyzed by flow cytometry of treated cells were shown. (E) and (F) Peritoneal macrophages were pretreated with indicated concentration of SMU-CX24 (0.1 and 1 μmol/L) and subjected to oxLDL (50 μg/mL) exposure for 2 h. Total RNA of treated cells were harvested and gene expression of (E) inflammatory cytokine *IL-6*, *IL-1β*, and (F) cholesterol efflux *Abca1* and *Abcg1* were analyzed. Data are expressed as the mean ± SD of three independent experiments. Statistical significance was determined using unpaired two-tailed Student's *t* test. $^{*}P < 0.05$; $^{**}P < 0.01$; $^{***}P < 0.001$; ns denotes not significant *versus* control treated with Poly I:C or ox-LDL.

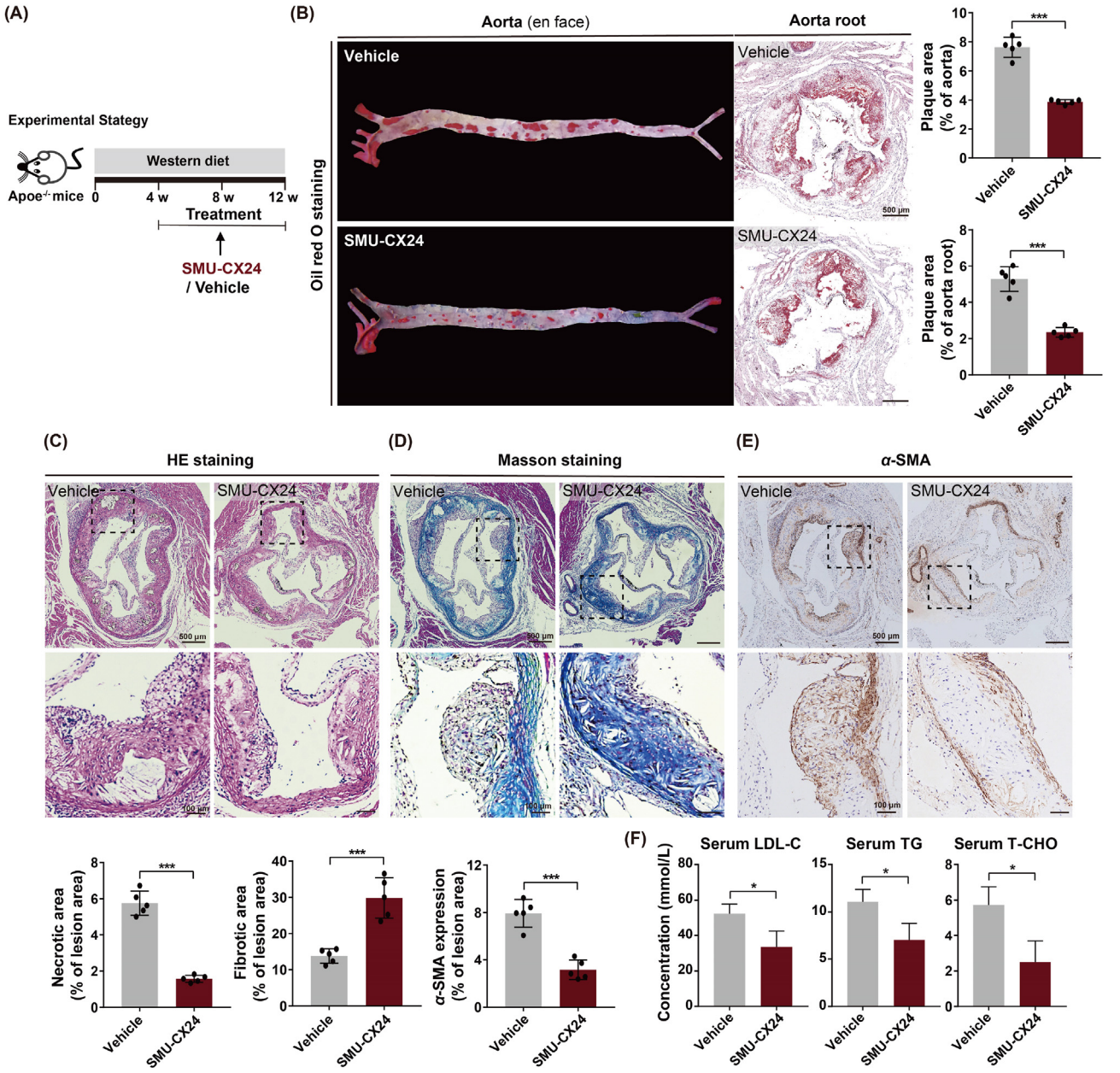

Figure 6 Atherosclerotic burden was significantly diminished in SMU-CX24-treated, Western diet-fed ApoE$^{-/-}$ mice. (A) Schematic illustration showed ApoE$^{-/-}$ mice were fed with a cholesterol-rich diet for 12 weeks and concomitantly treated with SMU-CX24 (5 mg/kg) or vehicle every 48 h by intraperitoneal injection during the last 8 weeks. (B) Representative images (left) and quantitative analysis (right) of oil red O staining of en face *in-situ* aortas and histological cross-sections of aortic root isolated from treated mice ($n = 5$ per group). (C–E) Representative images (top) and quantitative analysis (bottom) of aortic roots indicated to (C) H&E staining (dotted lines indicate the necrotic area), (D) Masson staining and (E) immunohistochemical staining of an antibody against α-SMA ($n = 5$ per group). (F) Serum lipid levels of LDL-C, TG and T-CHO from treated mice were analyzed ($n = 8$ per group). The data are expressed as the mean ± SD. Statistical significance was determined using unpaired two-tailed Student's *t* test. $^{*}P < 0.05$; $^{**}P < 0.01$; $^{***}P < 0.001$ *versus* the control treated with vehicle.

CX24 treated mice liver tissue at the transcription and translation levels (Fig. 7I). These data indicated that SMU-CX24-mediated TLR3 inhibition also affected the lipid accumulation in liver lesion. In summary, this evidence demonstrated that SMU-CX24 alleviated the atherogenic burden by exerting its TLR3 inhibitory effect to reduce inflammatory response within atherosclerotic lesions, providing solid evidence and support for TLR3-specific inhibitors in atherosclerosis treatment due to its anti-inflammatory effects.

3.7. *Pharmacokinetic properties of SMU-CX24*

Finally, we investigated the pharmacokinetic profiles of SMU-CX24 in SD rats. After a single intravenous injection (i.v.) of 8 mg/kg or oral administration (i.g.) of 24 mg/kg SMU-CX24, blood samples were collected from the orbital vein at the indicated time points (0, 5, 10, 15, 30, 60, 120, 240, 480, 720 and 1440 min) in heparin sodium coated microtubes. The plasma concentration-time profiles of SMU-CX24 with the different administration procedures were shown in

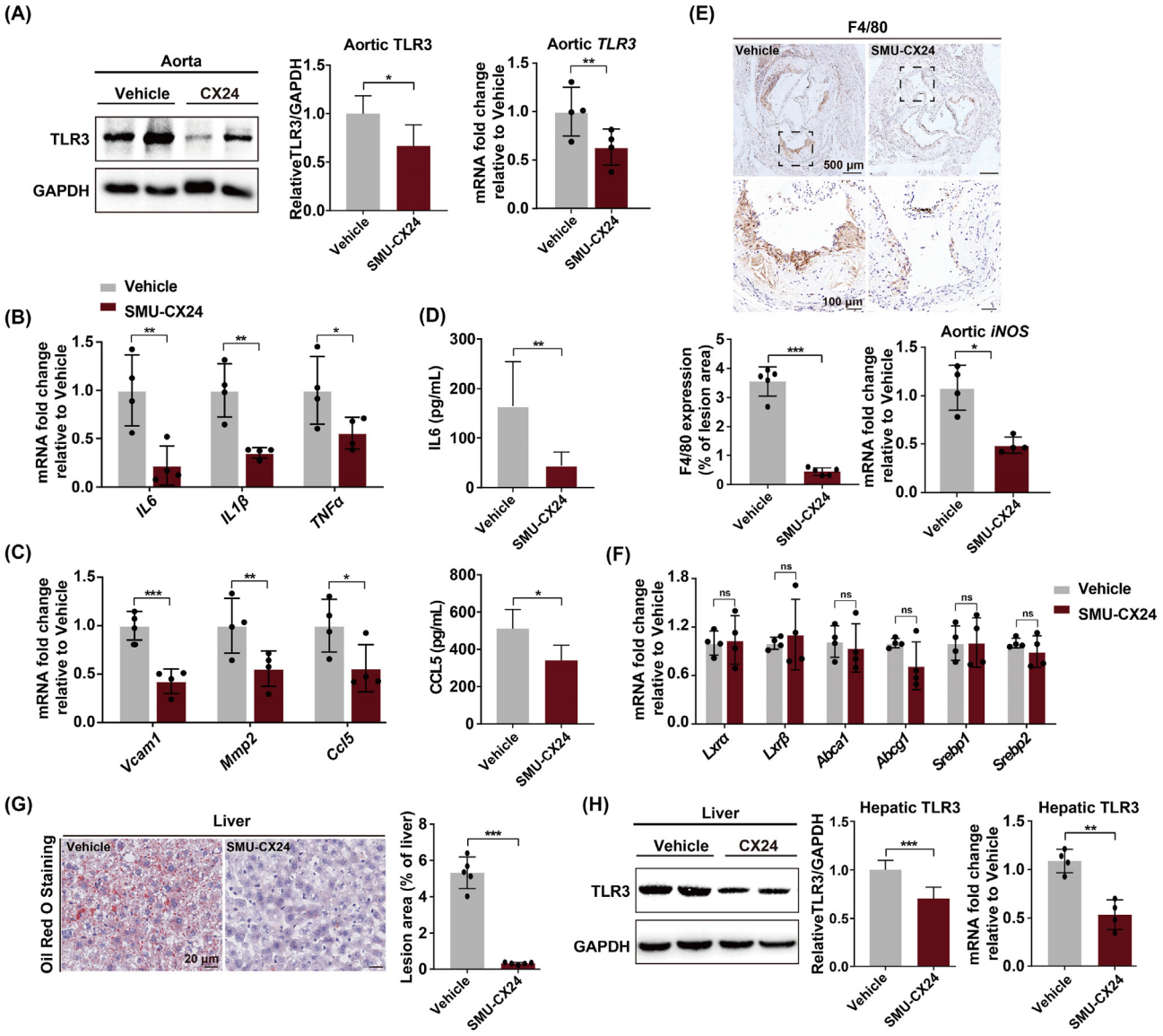

Figure 7 Inflammatory response was significantly decreased in SMU-CX24 treated, Western diet-fed ApoE$^{-/-}$ mice. (A) Protein and gene expression of TLR3 in the aorta from SMU-CX24 and vehicle treated mice were analyzed ($n = 4$ per group). (B) and (C) Gene expression of (B) inflammatory cytokines of *TNFα*, *IL6* and *IL1β*, and (C) atherogenic cytokine of *Vcam1*, *Ccl5* and *Mmp2* of aorta from treated mice were analyzed ($n = 4$ per group). (D) Serum concentration of IL-6 and CCL5 of treated mice were shown ($n = 8$ per group). (E) Representative images (top) and quantitative analysis (bottom) of aortic roots stained with an antibody against F4/80 ($n = 5$ per group) were shown. Gene expression of M1 macrophages marker *INOS* of aorta from treated mice were analyzed ($n = 4$ per group). (F) Gene expression of cholesterol efflux associated genes of aorta from treated mice, including *Lxrα*, *Lxrβ*, *Abca1*, *Abcg1*, *Srebp1* and *Srebp2*, were analyzed ($n = 4$ per group). (G) Representative images (left) and quantitative analysis (right) of histological cross-sections of liver tissue stained with oil red O ($n = 4$ per group) were shown. (H) Protein and gene expression of TLR3 in the liver from treated mice were analyzed ($n = 4$ per group). The data are expressed as the mean ± SD. Statistical significance was determined using unpaired two-tailed Student's *t* test. *$P < 0.05$; **$P < 0.01$; ***$P < 0.001$ *versus* the control treated with vehicle.

Supporting Informaion Fig. S11A and B. Table 1 summarizes the primary pharmacokinetic parameters of SMU-CX24. Briefly, the long half-life of SMU-CX24 after i.v. injection and oral administration was calculated as 5.05 ± 2.64 and 10.71 ± 0.60 h, respectively, with a $t_{1/2}$ (i.g.)/$t_{1/2}$ (i.v.) ratio of 2.12, exhibiting a close metabolic rate for SMU-CX24 *via* oral administration (i.g.) compared to i.v. injection. The absolute oral bioavailability of SMU-CX24 was calculated as 22.64%, indicating a reasonable pharmacokinetic property after being dissolved in disodium citrate phosphate buffer, which shows potential for its future clinical use.

4. Discussion

Atherosclerosis (AS) is characterized by excessive cholesterol deposition in the vessel wall and subsequent chronic inflammation

Table 1 The pharmacokinetic parameters of SMU-CX24 after intravenous (i.v.) and oral (i.g.) administration to SD rats ($n = 5$ per group).

Parameters	Unit	Intravenous injection (i.v., 8 mg/kg)	Oral administration (i.g., 24 mg/kg)
T_{max}	H	0.14 ± 0.08	4.00
C_{max}	μg/L	430.56 ± 167.43	46.42 ± 16.59
$t_{1/2}$	H	5.05 ± 2.64	10.71 ± 0.60
AUC_{0-t}	μg/L·h	963.53 ± 165.45	411.03 ± 40.93
$AUC_{0-\infty}$	μg/L·h	1001.90 ± 149.83	531.21 ± 62.80
F	%		22.64 ± 0.91

The data are expressed as the mean ± SD.

enriched in atherosclerotic lesions[38]. Mechanisms involved in the resolution of inflammation contribute to disease alleviation[7]. Currently, pharmacological treatment with statins is recommended as a first-line treatment to modulate cholesterol content and prevents of atherosclerosis and cardiovascular diseases development[39,40]. However, for people who are tolerant to statins or have serious inflammation, statin treatment seemed to have limited therapeutic efficacy[39,41]. Inflammatory responses are sustained and affect continued the entire process of atherosclerosis, indicating the feasibility of personalized or combined therapeutics in treating AS combined with anti-inflammatory therapies. Currently, immunosuppressive strategies, such as the use of using anti-inflammatory modulators targeting IL1β and vaccines, have been explored to treat atherosclerosis[42–44].

TLR3 is suggested to be involved in the atherosclerotic process by initiating inflammatory and atherogenic effects, while studies of the athero-protective role of TLR3 *via* diverse mechanisms have also been reported[45–47]. These diverse descriptions may be ascribed to different mechanisms or models. For example, Cole et al.[47] indicated the protective role of TLR3 in the formation of early atherosclerotic lesions in mice fed a standard chow diet, which differed from other established studies that used a cholesterol rich Western diet and adult mice to mimic the events of atherosclerosis[20]. Herein, we ascertained the presence of TLR3 in human atherosclerotic lesion, which indicated that TLR3 was involved in atherosclerosis regulation. A significant increase in the expression of TLR3 in atherosclerotic PBMCs was also consistent with our hypothesis, suggesting the inflammation-mediated proatherogenic function of TLR3. Here, we also observed that activation of TLR3 induced a dramatic increase in the expression of atherogenic chemokines (CCL2 and CCL5) and adhesion molecules (VCAM-1 and ICAM-1) in mice, while gene silencing of *TLR3* hindered foam cell formation. Collectively, in this study, the evidence indicated that TLR3 involved in atherosclerosis regulation, and we considered pharmacological intervention with TLR3 to be an alternate therapeutic strategy for atherosclerosis. However, the lack of specific TLR3 inhibitors precluded the associated previous studies.

Due to complex interactions between dsRNA-TLR3, only a few TLR3 modulators have been studied extensively due to their poor efficacy and bioavailability[48]. In this study, based on a high-throughput cell-based screening method, we identified the TLR3 inhibitory function of the carbazole alkaloid 9-methoxy elliciptine NSC69187 (CX1), which originated from *O. elliptica*. Since CX1 lacks structural novelty and has poor bioavailability, we subsequently performed several chemical modifications using CX1 as a parent compound. We ultimately identified and synthesized the novel compound SMU-CX24 with a $-CH_2NHCH(CH_3)_2$ substitution at the 9th position in the CX1 structure, which was tenfold more effective in inhibiting TLR3 than the parent compound CX1 and had increased aqueous solubility and a remarkable pharmacokinetic profile. SMU-CX24 exerted its anti-inflammatory effect by mediating pharmacological intervention of TLR3 expression in atherosclerotic lesion of aorta and liver, and proven to have atherosclerosis alleviation and protection in a western diet feeding atherosclerotic model. Interesting, SMU-CX24 was observed to decrease M1 pro-inflammatory macrophage and inflammation infiltration within aortic lesion area, while no apparent of expression changes in macrophages-modulated cholesterol efflux by liver X receptor-dependent gene, which further indicated the inflammation-mediated anti-atherosclerosis effect of SMU-CX24 on atherosclerosis.

Based on SAR studies, it is clear that both the indole and isoquinoline rings are indispensable for the majority of TLR3 inhibitor activity. Therefore, we focused on the substitutes at the 9th position and *N*-alkylated compounds. Our newly synthesized SMU-CX24 has significantly increased TLR3 inhibitory activity and very good aqueous solubility, which might be due to the substituted side chain, which enhanced the alkalinity of the compound to form a salt with an acid. This property could also be the reason for the increased binding to TLR3 within a weak acidic endosomal environment[49]. Since the TLR3 ligand Poly I:C also elicits inflammatory responses *via* RIG-1 and MDA5 receptors, we used transfected HEK-Blue hTLR3 cells to further confirm the TLR3 specificity of the SMU-CX24 compound. In addition, we showed direct, high affinity binding of SMU-CX24 to the TLR3, while the negative control was negligible to bind to TLR3. We preliminary explored the binding mode of TLR3 and SMU-CX24, and we surprised to find that SMU-CX24 compete to bind to TLR3 with Poly I:C, which was similar to the available used TLR3 inhibitor CU-CPT 4a[28]. In this study, for the first time, we documented a strong fluorescence property of SMU-CX24, similar to that of the antitumor drug camptothecin[50]. Hence, apart from identifying drug intake capability in the current study, further application of SMU-CX24 as a molecular probe in biology research is quite promising.

In conclusion, a clinical link between TLR3 activation and atherosclerosis was revealed. We identified, synthesized and evaluated the novel TLR3-specific inhibitor SMU-CX24, which has an IC_{50} value of 18.87 ± 2.21 nmol/L. For the first time, SMU-CX24 was shown to alleviate atherosclerosis and protect against atherosclerosis by pharmacological intervention with TLR3. Hence, SMU-CX24 is a novel therapeutic agent for translational research and treatment of atherosclerosis.

Acknowledgments

This study was supported by National Natural Science Foundation of China (Nos. 81773558, 82073689 (KC), and 1825702 (HY)), National Natural Science Foundation of Guangdong Province (Nos. 2020A151501518, 2018B030312010, China) and Science and Technology Program of Guangzhou (No. 201904010380, China).

Author contributions

Conceptualization: Xiaohong Cen, Kui Cheng, Shuwen Liu and Hang Yin; Designed and performed researches: Xiaohong Cen, Baoqu Wang, Yuqing Liang, Yu Xiao and Kui Cheng; Data

analysis: Xiaohong Cen, Baoqu Wang, Yuqing Liang, Yanlin Chen, Yu Xiao, Shaohua Du and Kui Cheng; Manuscript writing, reviewing and editing: Xiaohong Cen, Kutty Selva Nandakumar, Kui Cheng, Shuwen Liu and Hang Yin.

Conflicts of interest

The authors declare no conflicts of interest.

Appendix A. Supporting information

Supporting data to this article can be found online at https://doi.org/10.1016/j.apsb.2022.06.001.

References

1. Jaipersad AS, Lip GY, Silverman S, Shantsila E. The role of monocytes in angiogenesis and atherosclerosis. *J Am Coll Cardiol* 2014;**63**:1−11.
2. Koelwyn GJ, Corr EM, Erbay E, Moore KJ. Regulation of macrophage immunometabolism in atherosclerosis. *Nat Immunol* 2018;**19**:526−37.
3. Depuydt MAC, Prange KHM, Slenders L, Örd T, Elbersen D, Boltjes A, et al. Microanatomy of the human atherosclerotic plaque by single-cell transcriptomics. *Circ Res* 2020;**127**:1437−55.
4. Gisterå A, Hansson GK. The immunology of atherosclerosis. *Nat Rev Nephrol* 2017;**13**:368−80.
5. Takeuchi O, Akira S. Pattern recognition receptors and inflammation. *Cell* 2010;**140**:805−20.
6. Gong T, Liu L, Jiang W, Zhou R. DAMP-sensing receptors in sterile inflammation and inflammatory diseases. *Nat Rev Immunol* 2020;**20**:95−112.
7. Bäck M, Yurdagul Jr A, Tabas I, Öörni K, Kovanen PT. Inflammation and its resolution in atherosclerosis: mediators and therapeutic opportunities. *Nat Rev Cardiol* 2019;**16**:389−406.
8. Pryshchep O, Ma-Krupa W, Younge BR, Goronzy JJ, Weyand CM. Vessel-specific toll-like receptor profiles in human medium and large arteries. *Circulation* 2008;**118**:1276−84.
9. Mann DL. Innate immunity and the failing heart: the cytokine hypothesis revisited. *Circ Res* 2015;**116**:1254−68.
10. Tang X, Pan L, Zhao S, Dai F, Chao M, Jiang H, et al. SNO-MLP (*S*-nitrosylation of muscle LIM protein) facilitates myocardial hypertrophy through TLR3 (toll-like receptor 3)-mediated RIP3 (receptor-interacting protein kinase 3) and NLRP3 (NOD-like receptor pyrin domain containing 3) inflammasome activation. *Circulation* 2020;**141**:984−1000.
11. Goulopoulou S, McCarthy CG, Webb RC. Toll-like receptors in the vascular system: sensing the dangers within. *Pharmacol Rev* 2016;**68**:142−67.
12. Choe J, Kelker MS, Wilson IA. Crystal structure of human toll-like receptor 3 (TLR3) ectodomain. *Science* 2005;**309**:581−5.
13. Bartok E, Hartmann G. Immune sensing mechanisms that discriminate self from altered self and foreign nucleic acids. *Immunity* 2020;**53**:54−77.
14. Tajbakhsh A, Bianconi V, Pirro M, Gheibi Hayat SM, Johnston TP, Sahebkar A. Efferocytosis and atherosclerosis: regulation of phagocyte function by microRNAs. *Trends Endocrinol Metab* 2019;**30**:672−83.
15. Shoeibi S. Diagnostic and theranostic microRNAs in the pathogenesis of atherosclerosis. *Acta Physiol* 2020;**228**:e13353.
16. York AG, Williams KJ, Argus JP, Zhou QD, Brar G, Vergnes L, et al. Limiting cholesterol biosynthetic flux spontaneously engages type I IFN signaling. *Cell* 2015;**163**:1716−29.
17. Castrillo A, Joseph SB, Vaidya SA, Haberland M, Fogelman AM, Cheng G, et al. Crosstalk between LXR and toll-like receptor signaling mediates bacterial and viral antagonism of cholesterol metabolism. *Mol Cell* 2003;**12**:805−16.
18. Blanc M, Hsieh WY, Robertson KA, Watterson S, Shui G, Lacaze P, et al. Host defense against viral infection involves interferon mediated down-regulation of sterol biosynthesis. *PLoS Biol* 2011;**9**:e1000598.
19. Xiao J, Li W, Zheng X, Qi L, Wang H, Zhang C, et al. Targeting 7-dehydrocholesterol reductase integrates cholesterol metabolism and IRF3 activation to eliminate infection. *Immunity* 2020;**52**:109−22.e6.
20. Zimmer S, Steinmetz M, Asdonk T, Motz I, Coch C, Hartmann E, et al. Activation of endothelial Toll-like receptor 3 impairs endothelial function. *Circ Res* 2011;**108**:1358−66.
21. Stawski L, Marden G, Trojanowska M. The activation of human dermal microvascular cells by poly(I:C), lipopolysaccharide, imiquimod, and ODN2395 is mediated by the Fli1/FOXO3A pathway. *J Immunol* 2018;**200**:248−59.
22. Lundberg AM, Ketelhuth DFJ, Johansson ME, Gerdes N, Liu S, Yamamoto M, et al. Toll-like receptor 3 and 4 signalling through the TRIF and TRAM adaptors in haematopoietic cells promotes atherosclerosis. *Cardiovasc Res* 2013;**99**:364−73.
23. Ishibashi M, Sayers S, D'Armiento JM, Tall AR, Welch CL. TLR3 deficiency protects against collagen degradation and medial destruction in murine atherosclerotic plaques. *Atherosclerosis* 2013;**229**:52−61.
24. Gillespie MA, Gold ES, Ramsey SA, Podolsky I, Aderem A, Ranish JA. An LXR-NCOA5 gene regulatory complex directs inflammatory crosstalk-dependent repression of macrophage cholesterol efflux. *EMBO J* 2015;**34**:1244−58.
25. Feingold KR, Shigenaga JK, Kazemi MR, McDonald CM, Patzek SM, Cross AS, et al. Mechanisms of triglyceride accumulation in activated macrophages. *J Leukoc Biol* 2012;**92**:829−39.
26. Federico S, Pozzetti L, Papa A, Carullo G, Gemma S, Butini S, et al. Modulation of the innate immune response by targeting Toll-like receptors: a perspective on their agonists and antagonists. *J Med Chem* 2020;**63**:13466−513.
27. Cen X, Zhu G, Yang J, Yang J, Guo J, Jin J, et al. TLR1/2 Specific small-molecule agonist suppresses leukemia cancer cell growth by stimulating cytotoxic T lymphocytes. *Adv Sci* 2019;**6**:1802042.
28. Cheng K, Wang X, Yin H. Small-molecule inhibitors of the TLR3/dsRNA complex. *J Am Chem Soc* 2011;**133**:3764−7.
29. Wu P. Inhibition of RNA-binding proteins with small molecules. *Nat Rev Chem* 2020;**4**:441−58.
30. Liu L, Botos I, Wang Y, Leonard JN, Shiloach J, Segal DM, et al. Structural basis of toll-like receptor 3 signaling with double-stranded RNA. *Science* 2008;**320**:379−81.
31. Inamori K, Ariki S, Kawabata S. A Toll-like receptor in horseshoe crabs. *Immunol Rev* 2004;**198**:106−15.
32. Kato H, Takeuchi O, Sato S, Yoneyama M, Yamamoto M, Matsui K, et al. Differential roles of MDA5 and RIG-I helicases in the recognition of RNA viruses. *Nature* 2006;**441**:101−5.
33. Kizek R, Adam V, Hrabeta J, Eckschlager T, Smutny S, Burda JV, et al. Anthracyclines and ellipticines as DNA-damaging anticancer drugs: recent advances. *Pharmacol Ther* 2012;**133**:26−39.
34. Andrews WJ, Panova T, Normand C, Gadal O, Tikhonova IG, Panov KI. Old drug, new target: ellipticines selectively inhibit RNA polymerase I transcription. *J Biol Chem* 2013;**288**:4567−82.
35. Vehar B, Hrast M, Kova A, Konc J, Mariner K, Chopra I, et al. Ellipticines and 9-acridinylamines as inhibitors of D-alanine:D-alanine ligase. *Bioorg Med Chem* 2011;**19**:5137−46.
36. Kolattukudy PE, Niu J. Inflammation, endoplasmic reticulum stress, autophagy, and the monocyte chemoattractant protein-1/CCR2 pathway. *Circ Res* 2012;**110**:174−89.
37. Ruparelia N, Chai JT, Fisher EA, Choudhury RP. Inflammatory processes in cardiovascular disease: a route to targeted therapies. *Nat Rev Cardiol* 2017;**14**:133−44.
38. Wolf D, Ley K. Immunity and inflammation in atherosclerosis. *Circ Res* 2019;**124**:315−27.
39. Ray KK, Corral P, Morales E, Nicholls SJ. Pharmacological lipid-modification therapies for prevention of ischaemic heart disease: current and future options. *Lancet* 2019;**394**:697−708.

40. Soppert J, Lehrke M, Marx N, Jankowski J, Noels H. Lipoproteins and lipids in cardiovascular disease: from mechanistic insights to therapeutic targeting. *Adv Drug Deliv Rev* 2020;**159**:4−33.
41. Libby P, Everett BM. Novel antiatherosclerotic therapies. *Arterioscler Thromb Vasc Biol* 2019;**39**:538−45.
42. Nilsson J, Hansson GK. Vaccination strategies and immune modulation of atherosclerosis. *Circ Res* 2020;**126**:1281−96.
43. Abbate A, Toldo S, Marchetti C, Kron J, Van Tassell BW, Dinarello CA. Interleukin-1 and the inflammasome as therapeutic targets in cardiovascular disease. *Circ Res* 2020;**126**:1260−80.
44. Ridker PM, MacFadyen JG, Thuren T, Everett BM, Libby P, Glynn RJ. Effect of interleukin-1β inhibition with canakinumab on incident lung cancer in patients with atherosclerosis: exploratory results from a randomised, double-blind, placebo-controlled trial. *Lancet* 2017;**390**:1833−42.
45. Cherepanova OA, Gomez D, Shankman LS, Swiatlowska P, Williams J, Sarmento OF, et al. Activation of the pluripotency factor OCT4 in smooth muscle cells is atheroprotective. *Nat Med* 2016;**22**:657−65.
46. Sayed N, Wong WT, Ospino F, Meng S, Lee J, Jha A, et al. Transdifferentiation of human fibroblasts to endothelial cells: role of innate immunity. *Circulation* 2015;**131**:300−9.
47. Cole JE, Navin TJ, Cross AJ, Goddard ME, Alexopoulou L, Mitra AT, et al. Unexpected protective role for Toll-like receptor 3 in the arterial wall. *Proc Natl Acad Sci U S A* 2011;**108**:2372−7.
48. Rodrigues T, Reker D, Schneider P, Schneider G. Counting on natural products for drug design. *Nat Chem* 2016;**8**:531−41.
49. Liu S, Jiang Q, Zhao X, Zhao R, Wang Y, Wang Y, et al. A DNA nanodevice-based vaccine for cancer immunotherapy. *Nat Mater* 2021;**20**:421−30.
50. Hao Y, Chen Y, He X, Yu Y, Han R, Li Y, et al. Polymeric nanoparticles with ROS-responsive prodrug and platinum nanozyme for enhanced chemophotodynamic therapy of colon cancer. *Adv Sci* 2020;**7**:2001853.